CD44 anchors the assembly of matrilysin/MMP-7 with heparin-binding epidermal growth factor precursor and ErbB4 and regulates female reproductive organ remodeling

Wei-Hsuan Yu, J. Frederick Woessner, Jr.,[1] John D. McNeish,[2] and Ivan Stamenkovic[3]

Molecular Pathology Unit, Massachusetts General Hospital, and Department of Pathology, Harvard Medical School, Boston, Massachusetts 02129, USA; [1]Department of Biochemistry and Molecular Biology, University of Miami School of Medicine, Miami, Florida 33101, USA; [2]Pfizer Central Research, Groton, Connecticut 06340, USA

CD44 is a facultative proteoglycan implicated in cell adhesion and trafficking, as well as in tumor survival and progression. We demonstrate here that CD44 heparan sulfate proteoglycan (CD44HSPG) recruits proteolytically active matrix metalloproteinase 7 (matrilysin, MMP-7) and heparin-binding epidermal growth factor precursor (pro-HB-EGF) to form a complex on the surface of tumor cell lines, postpartum uterine and lactating mammary gland epithelium, and uterine smooth muscle. The HB-EGF precursor within this complex is processed by MMP-7, and the resulting mature HB-EGF engages and activates its receptor, ErbB4, leading to, among other events, cell survival. In CD44$^{-/-}$ mice, postpartum uterine involution is accelerated and maintenance of lactation is impaired. In both uterine and mammary epithelia of these mice, MMP-7 localization is altered and pro-HB-EGF processing as well as ErbB4 activation are decreased. Our observations provide a mechanism for the assembly and function of a cell surface complex composed of CD44HSPG, MMP 7, HB-EGF, and ErbB4 that may play an important role in the regulation of physiological tissue remodeling.

[*Key Words:* CD44; MMP-7; HB-EGF; ErbB4; complex; remodeling]

Received July 3, 2001; revised version accepted December 10, 2001.

The highly polymorphic facultative cell surface proteoglycan CD44 is implicated in a variety of cellular functions, including adhesion, migration, activation, invasion, and survival (for review, see Lesley et al. 1993). Several of these functions have been attributed to the ability of CD44 to bind hyaluronan (HA; Aruffo et al. 1990; Stamenkovic et al. 1991), for which CD44 appears to be a major cell surface receptor. However, there is strong evidence that variant exon usage and cell type-specific glycosylation endow CD44 with additional properties. CD44 isoforms containing the variant exon v3 (Screaton et al. 1992) display both biochemical and functional characteristics of heparan sulfate proteoglycans (HSPGs; Bennett et al. 1995). The v3 exon contains Ser-Gly repeats that support covalent attachment of high molecular weight HS side chains (Bartolazzi et al. 1995; Bennett et al. 1995), which bind selected heparin-binding growth factors, including basic fibroblast growth factor (bFGF), heparin-binding epidermal growth factor (HB-EGF; Bennett et al. 1995), and FGF-8 (Sherman et al. 1998). The physiological relevance of these interactions has remained largely obscure, and although it has been suggested that CD44v3 HSPG, henceforth referred to as CD44HSPG, may present these growth factors to their specific receptors (Bennett et al. 1995; Sherman et al. 1998), no direct evidence of CD44HSPG participation in such events in vivo has been provided thus far. Nevertheless, we have observed that CD44-deficient mouse keratinocytes fail to proliferate in response to HB-EGF (Kaya et al. 1997), rendering conceivable the notion that CD44HSPG provides a mechanism for the presentation of HB-EGF to its receptors.

Interaction of mature HB-EGF with HSPG, via its heparin-binding domain, is required for optimal binding to its receptors (Higashiyama et al. 1993), which belong to the ErbB subclass of receptor tyrosine kinases (for review, see Olayioye et al. 2000). Engagement of ErbB receptors by HB-EGF is implicated in wound healing (Marikovsky et al. 1993), cell proliferation and migration (Higashiyama et al. 1993), blastocyst implantation (Raab et al. 1996), and protection from apoptotic cell death

[3]Corresponding author.
E-MAIL stamenko@helix.mgh.harvard.edu; FAX (617)726-5684.
Article and publication are at http://www.genesdev.org/cgi/doi/10.1101/gad.925702.

(Opanashuk et al. 1999). All six of the known mammalian EGF-related molecules, including EGF, HB-EGF, transforming growth factor alpha (TGF-α), amphiregulin, betacellulin, and epiregulin are expressed as integral membrane precursor proteins (Olayioye et al. 2000). Their activation requires proteolytic removal of the propeptide, and release of the corresponding mature protein from the cell surface, which can bind or be presented to ErbB receptors (Olayioye et al. 2000). Although the mechanisms that underlie the processing of most EGF family precursors remain unknown, recent evidence suggests that matrix metalloproteinases (MMPs) are involved in the proteolytic cleavage of the HB-EGF precursor (Suzuki et al. 1997; Izumi et al. 1998; Prenzel et al. 1999). This notion is based on the observation that release of mature HB-EGF from the cell surface is abrogated by most hydroxamate-based synthetic MMP inhibitors or divalent cation chelating reagents (Suzuki et al. 1997; Prenzel et al. 1999).

Matrix metalloproteinases and ADAMs are two of the four subfamilies of the metzincins, which are believed to play key roles in orchestrating both physiological and pathological mammalian tissue remodeling (Werb 1997; Lukashev and Werb 1998; Shapiro 1998; Nagase and Woessner 1999). There are currently 24 identified MMPs, most of which are expressed in secreted form, whose combined activity can degrade all of the extracellular matrix (ECM) proteins (Bode et al. 1996; Vu and Werb 2000). In addition to ECM proteins, MMPs can proteolytically activate a variety of ECM- and membrane-bound latent growth factors and cleave cell surface adhesion receptors (for review, see Murphy and Gavrilovic 1999; Bergers and Coussens 2000). Several reports suggest that cell surface docking of secreted MMPs may be required for their ability to promote ECM degradation and latent growth factor processing (Brooks et al. 1996; Chen 1996; Yu and Stamenkovic 2000). Recently, heparan sulfate proteoglycans have been proposed to provide a cell surface docking mechanism for matrilysin/MMP-7, based on the observation that MMP-7 displays high affinity for heparan sulfate glycosaminoglycans (GAGs, Yu and Woessner 2000).

MMP-7 is the smallest known secreted MMP and lacks the C-terminal hemopexin homology domain, which is believed to participate in promoting MMP interaction with substrate (Nagase and Woessner 1999). It is therefore plausible that optimal interaction between MMP-7 and its substrates requires the intervention of a third molecule, such as an HSPG, that serves to recruit both enzyme and substrate to the same site. Matrilysin/MMP-7 is expressed on the apical surface of intestinal mucosal, endometrial and glandular epithelial cells, as well as in carcinomas and mononuclear phagocytic cells (Woessner 1996), all of which constitutively or inducibly express CD44HSPG (for review, see Lesley et al. 1993). Functionally, MMP-7 is implicated in physiological ECM remodeling during reproductive organ involution (Woessner 1996; Yu and Woessner 2000), host defense (Wilson et al. 1999), and tumor survival (Witty et al. 1994; Wilson et al. 1997; Rudolph-Owen et al. 1998).

Here, we address the possibility that CD44HSPG might direct the assembly of MMP-7, HB-EGF precursor, and the HB-EGF receptor ErbB4, and thereby provide a mechanism for the regulation of HB-EGF processing and function and physiological tissue remodeling.

Results

CD44HSPG recruits MMP-7 to the cell surface in complex in a broad range of cell types

To determine whether CD44HSPG provides a cell surface docking mechanism for MMP-7 we addressed the putative interaction between the two molecules in several cell types. Following phorbolester stimulation, neuroblastoma SH-SY5Y cells were observed to express CD44HSPG and MMP-7, which colocalized on the cell surface and along neurite extensions, as assessed by immunofluorescence microscopy of cells labeled with anti-CD44 and anti-MMP-7 antibody (Fig. 1A, top panel). Similar colocalization was observed when green fluorescence protein (GFP)-tagged MMP-7 and v5-his-tagged CD44v3-10 were transiently expressed in these cells in the absence of phorbolester stimulation (data not shown). Introduction of cDNAs encoding human CD44v3-10 and MMP-7 into CHO cells resulted in the colocalization of CD44HSPG and MMP-7 at the tips of cellular processes (Fig. 1A, bottom panel). Such colocalization was not observed when cDNAs encoding CD44 isoforms that do not contain the v3 exon were cotransfected with MMP-7 (data not shown). To determine whether colocalization of CD44HSPG and MMP-7 is heparan sulfate-dependent, Ltk– [L-M(TK–)] cells were transfected with a cDNA encoding CD44v3-10 and tested for their ability to bind exogenous MMP-7 (containing a E219Q mutation that abrogates catalytic activity) in the presence and absence of a heparin wash (Fig. 1B). MMP-7 bound poorly to the surface of Ltk– cells but strongly to Ltk– transfectants expressing CD44v3-10. Binding was abolished by washing the transfectants with 0.2 mg/mL heparin (Fig. 1B).

We next addressed the colocalization and possible interaction among CD44HSPG, MMP-7, proHB-EGF, and ErbB4. We selected Namalwa B lymphoma cells for these experiments because they express MMP-7, HB-EGF, and ErbB4 but not CD44 (Sy et al. 1991; Bartolazzi et al. 1995). Based on the observed CD44HSPG–MMP-7 colocalization in three different cell types, we reasoned that if CD44HSPG orchestrates the assembly of MMP-7, HB-EGF, and ErbB4, the event should be general rather than cell type-specific, and introduction of the appropriate CD44 isoform into Namalwa cells should reconstitute the complex on the cell surface. In wild type Namalwa cells, MMP-7 expression was observed to be intracellular (data not shown). Stable expression of CD44HSPG in these cells resulted not only in the intracellular colocalization of CD44 and MMP-7, but also in the localization of MMP-7 to the cell surface (Fig. 2A, top panel). In contrast, CD44 isoforms that do not contain the v3 exon and lack high molecular weight HS, including CD44H (Fig.

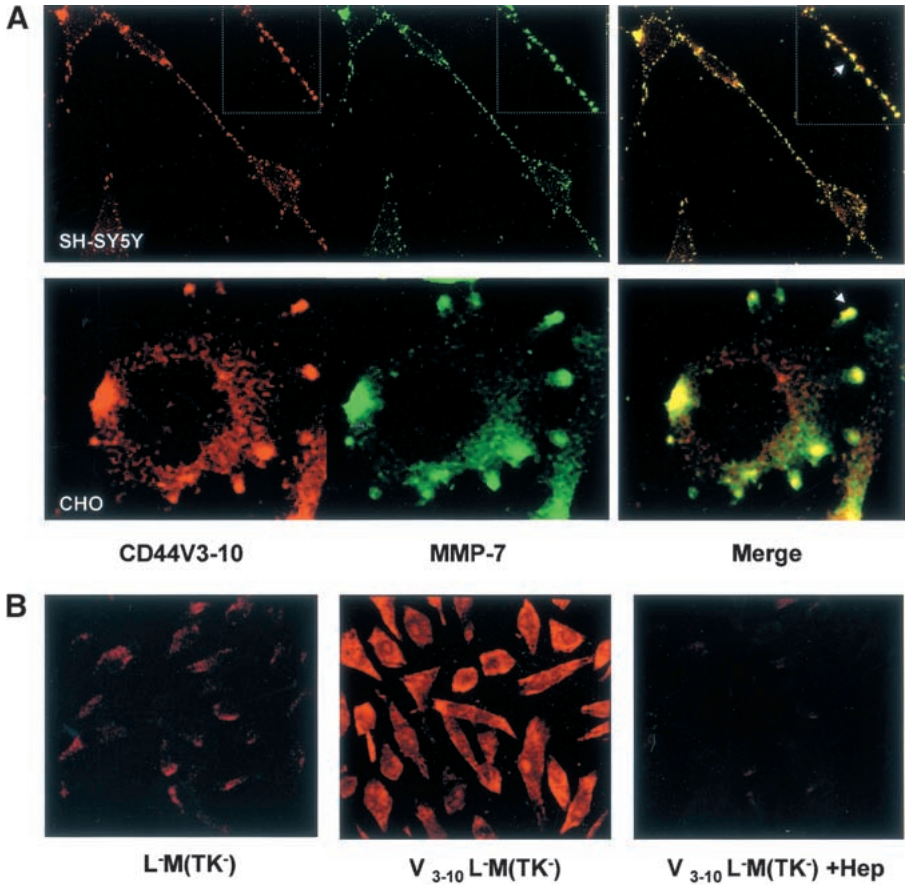

Figure 1. Colocalization of CD44HSPG and MMP-7 in cell lines. (*A*) (*Top* panel) Phorbolester-treated neuroblastoma SH-SY5Y cells display colocalization of MMP-7 and CD44HSPG on the cell surface and along neurite extensions (inset). (*Bottom* panel) CHO cells cotransfected with cDNAs encoding human CD44v3-10 and MMP-7 display colocalization of the two molecules in cell protrusions. (*B*) Recombinant purified MMP-7 binds weakly to Ltk– [L-M(TK$^-$)] cells, but strongly to Ltk– cells transfected with CD44v3-10. Binding is abrogated by washing the transfectants with 0.2 mg/mL heparin.

2A, bottom panel) and CD44v7-10 (data not shown) failed to localize MMP-7 to the cell surface.

To verify the formation of a CD44HSPG–MMP-7 complex on the surface of Namalwa transfectants, coimmunoprecipitation experiments were performed, in which cells were incubated with an anti-MMP-7 polyclonal antibody (RM7-C; Yu and Woessner 2000), raised against a unique C-terminal MMP-7 peptide prior to lysis in a 0.5% Triton-X buffer. The RM7-C antibody does not display cross reactivity with MMPs 1, 2, 3, 8, 9, and 13, fails to stain cells that do not express MMP-7 (Yu and Woessner 2000; data not shown), and its reactivity with Namalwa CD44HSPG transfectants was abrogated by the immunogenic peptide (data not shown). Following cell lysis, the immunoprecipitates were subjected to SDS-PAGE, transferred onto nitrocellulose membranes and immunoblotted with anti-CD44 mAb. Among the RM7-C antibody immunoprecipitates derived from Namalwa cells expressing different CD44 isoforms, only those from CD44HSPG transfectants contained CD44 (Fig. 2B), which appeared as a smear, consistent with the presence of high molecular weight HS chains (Bartolazzi et al. 1995). These observations support the notion that expression of the v3 exon/HS is required for CD44-MMP-7 complex formation.

To provide further evidence that CD44HSPG associates with MMP-7, heparin eluates of anti-CD44 mAb immunoprecipitates derived from CD44v3 transfectants were subjected to heparin-enhanced CM-transferrin zymogram analysis (Yu and Woessner 2000). Active MMP-7, as indicated by its molecular weight (Yu and Woessner 2000), could be heparin-eluted from anti-CD44 mAb immunoprecipitates of CD44v3 transfectants, and fully or partially removed from the CD44v3 complexes by heparitinase or chondroitin lyase ABC treatment, respectively (Fig. 2C). Heparin eluates of immunoprecipitates of CD44 isoforms that lack the v3 exon, and the associated HS, did not display MMP-7 activity on CM-transferrin zymogams (data not shown). These observations not only support the notion that CD44HSPG provides a docking mechanism for MMP-7, but also suggest that most of the MMP-7 associated with CD44HSPG has undergone cleavage of its pro-domain and is proteolytically active.

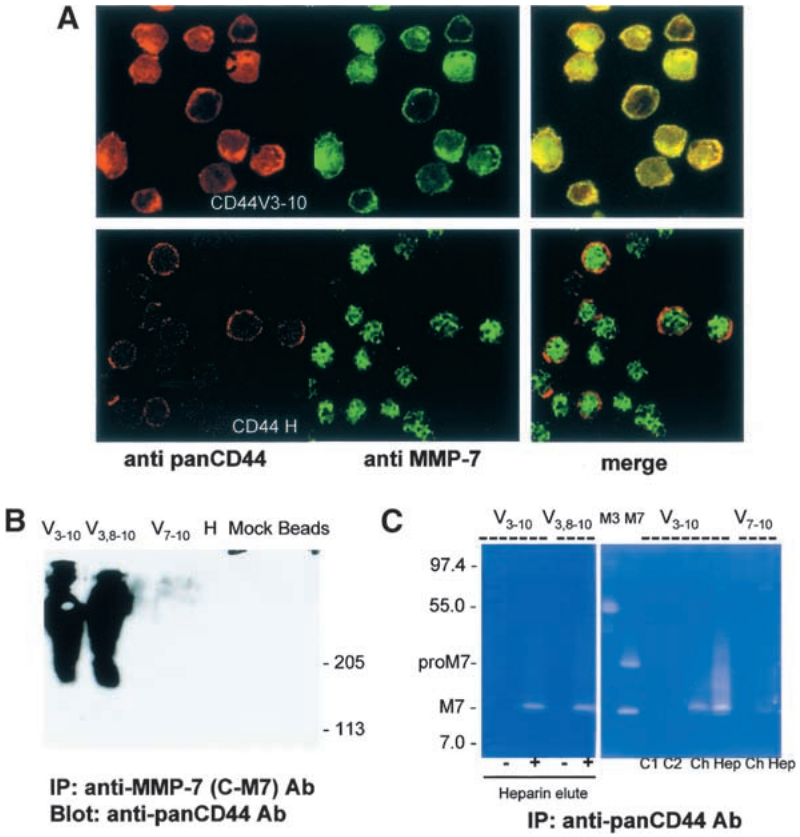

Figure 2. Reconstitution of the CD44HSPG/MMP 7/HB-EGF/ErB4 complex in Namalwa cells. (*A*) Confocal microscopy of Namalwa CD44 transfectants incubated with anti-CD44 (red fluorescence) and anti-MMP-7 (green fluorescence) mAb. Namalwa transfectants expressing CD44v3-10 (*top*) and CD44H (*bottom*) are shown. (*B*) Coimmunoprecipitation of CD44v3 and MMP-7. Indicated Namalwa transfectants were incubated with anti-MMP-7 C-M7 antibody, washed extensively, and lysed. Lysates were incubated with protein A sepharose beads and the immunoprecipitates were subjected to SDS-PAGE, transferred onto Hybond-C nitrocellulose membranes and immunoblotted with anti-CD44 mAb. (*C*) Transferrin zymogram of heparin eluates from anti-CD44 antibody immunoprecipitates of Namalwa CD44v3.8-10 and CD44v3-10 transfectant lysates (*left*). Transferrin zymogram of chondroitin lyase (Ch)– and heparanase (Hep)-treated anti-CD44 mAb immunoprecipitates from CD44v3-10 and CD44v7-10 Namalwa transfectants (*right*). C1 and C2 are control lanes containing protein A beads only (C1) and heparinase, chondroitinase, and digestion buffer in the absence of substrate (C2). MMP-3 (M3) and pro- and active-recombinant MMP-7 (M7) are used as marker controls. Migration of pro- and active MMP-7 are indicated on the *left* along with the molecular weight markers.

Pro-HB-EGF forms a complex with CD44HSPG and is a substrate of MMP-7

CD44HSPG binds pro-HB-EGF (Bennett et al. 1995) and pro-HB-EGF is processed by MMP-type proteolytic activity (Prenzel et al. 1999). If CD44HSPG provides a cell surface docking mechanism for MMP-7, it is conceivable that MMP-7 may be implicated in pro-HB-EGF processing. Mature HB-EGF should then be detected on the surface of CD44HSPG transfectants but not on that of cells expressing other CD44 isoforms. Consistent with this notion, neutralizing anti-HB-EGF antibody that recognizes mature forms of HB-EGF but not pro-HB-EGF, reacted with the surface of CD44HSPG-expressing Namalwa cells but not with cells transfected with CD44v7-10 and other, HS-negative CD44 isoforms (Fig. 3A, top panel; data not shown). MMP-7 was observed to colocalize with pro-HB-EGF in CD44HSPG transfectants, as assessed by confocal microscopy (Fig. 3A, bottom panel).

To address the possible association between MMP-7 and HB-EGF in Namalwa transfectants, immunoprecipitation of MMP-7 was performed using a buffer containing high zinc concentration (50 μM) that inhibits its proteolytic activity (Woessner and Taplin 1988; Yu and Woessner 2000), and should therefore facilitate coimmunoprecipitation of enzyme and substrate. Western blot analysis of anti-MMP-7 antibody immunoprecipitates from CD44HSPG Namalwa transfectants, using the anti-HB-EGF mAb C-18 that recognizes the cytoplasmic tail of human pro-HB-EGF, revealed the presence of a single major protein of 28 kD (Fig. 3B). Coimmunoprecipitation of MMP-7 and pro-HB-EGF from cells expressing CD44 isoforms that do not contain the v3 exon was not observed (Fig. 3B).

To determine whether MMP-7 is implicated in pro-HB-EGF processing, pro-HB-EGF coimmunoprecipitated with CD44HSPG was subjected to MMP-7 proteolysis in vitro. Protein A-bound anti-panCD44 antibody immunoprecipitates from CD44v3 Namalwa transfectants were treated with an EDTA-containing buffer to remove associated MMP-7 and any other potential MMP activity. EDTA can partially denature MMPs by chelating Ca^{+2} and Zn^{+2}, and thereby disrupt their heparin-binding ability (Yu and Woessner 2000). The immunoprecipitates were then washed with PBS containing Mg^{+2} and Ca^{+2} to remove any remaining EDTA and incubated with purified, *Escherichia coli*-derived, recombinant active MMP-7, in the presence and absence of the synthetic MMP inhibitor SC44463 whose IC:50 for MMP-7 is 10 nM (Butler et al. 1991; Abramson and Woessner 1994; Yu and Woessner 2000). In the presence of the inhibitor, as in the absence of MMP-7, immunoblotting with a combination of neutralizing anti-HB-EGF and C-18 anti-pro-HB-EGF antibodies, revealed three major species of HB-EGF with a molecular weight ranging between 22 and 28 kD (Fig. 3C). The 28-kD species corresponds to that of pro-HB-EGF coimmunoprecipitated with MMP-7 (Fig. 3B). In the absence of inhibitor, immunoblotting with

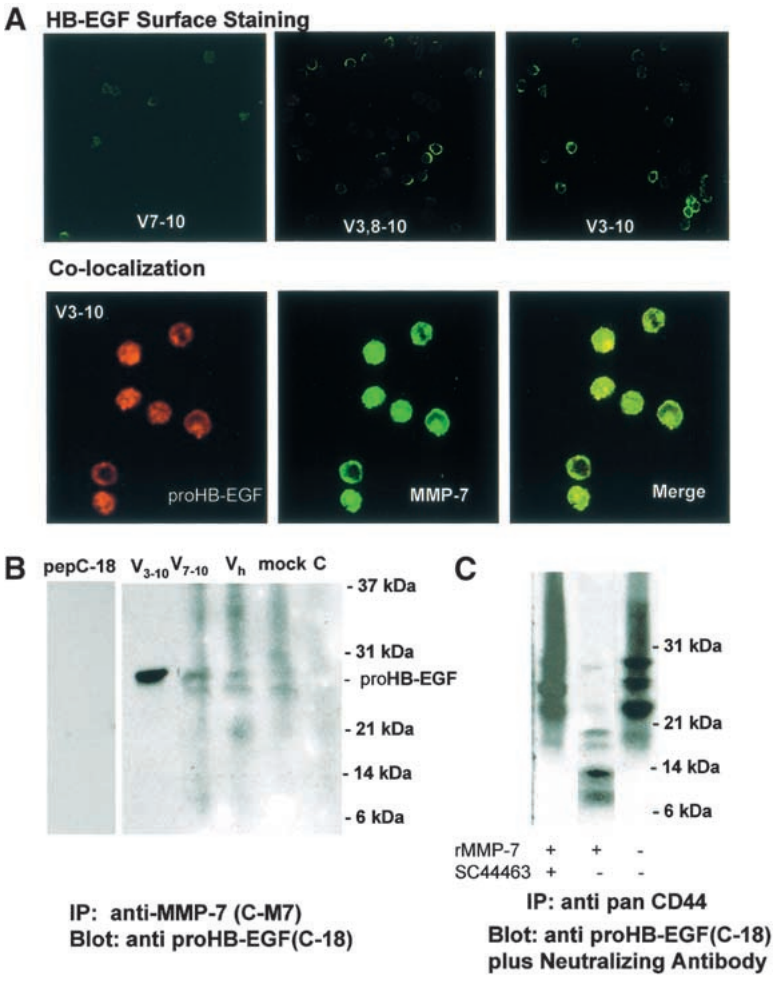

Figure 3. HB-EGF association with and processing by MMP 7. (*A*) (*Top* panel) Localization of HB-EGF on the surface of CD44v3 isoform expressing Namalwa cells, as assessed by neutralizing anti-HB-EGF antibody reactivity. (*Bottom* panel) Colocalization of proHB-EGF (C-18 antibody) and MMP-7 (RM7-C antibody) in Namalwa cells transfected with CD44v3-10, as assessed by confocal microscopy (magnification, 63×). (*B*) Coimmunoprecipitation of HB-EGF and MMP-7. MMP-7 was immunoprecipitated from Namalwa cells expressing the indicated CD44 isoforms with the indicated anti-MMP-7 antibody. The immunoprecipitates were subjected to SDS-PAGE, transferred onto nylon filters, and immunoblotted with the indicated anti-HB-EGF mAb. Lanes indicated pep C-18 and Mock C, respectively denote immunoprecipitates in the presence of immunogenic peptide and immunoprecipitates derived from vector only transfectants. (*C*) Proteolytic cleavage of pro-HB-EGF by MMP-7. Namalwa transfectant-derived anti-CD44 mAb immunoprecipitates were washed with a buffer containing EDTA to remove the coimmunoprecipitated MMP-7 and any other possibly associated MMP activity. The immunoprecipitates were then incubated with recombinant active MMP-7 in the presence or absence of the synthetic inhibitor SC44463 and subjected to SDS-PAGE, transfer to nitrocellulose membranes, and immunoblotting with a combination of neutralizing and cytoplasmic domain anti-HB-EGF mAb. Molecular weight markers are indicated.

the same two antibodies revealed at least four HB-EGF species of 10, 14, 18, and 19 kD (Fig. 3C). The size of these species is consistent with those believed to represent the active HB-EGF forms observed in the lysates and conditioned culture media of cells stimulated with phorbolester and kinaic acid (Opanashuk at al. 1999; Gechtman et al. 2000).

ErbB4 associates with several CD44 isoforms but is tyrosine phosphorylated predominantly when associated with CD44HSPG

The observations that CD44HSPG isoforms form a complex with MMP-7 and HB-EGF, and that pro-HB-EGF may be an MMP-7 substrate are consistent with the possibility that CD44HSPG may present the processed HB-EGF to its receptor(s). HB-EGF binds to the ErbB receptor tyrosine kinase family, and more specifically, to ErbB1 or ErbB4 (for review, see Olayioye et al. 2000). ErbB4 was observed to colocalize with a variety of CD44 isoforms in Namalwa transfectants (Fig. 4A). However, Western blot analysis of anti-CD44 antibody immunoprecipitates using anti-phosphotyrosine mAb, revealed tyrosine phosphorylation of ErbB4 (185 kD) predominantly in immunoprecipitates derived from CD44HSPG transfectants (Fig. 4B, top panel). Only minor ErbB4 tyrosine phosphorylation was observed in transfectants expressing non-v3 exon-containing CD44 isoforms, including CD44H, v6-10 and v7-10, even though ErbB4 was found to coimmunoprecipitate comparably with all of the CD44 variants tested (Fig. 4B, bottom panel). Pretreatment of cells with 50 ng/mL of neutralizing anti-HB-EGF antibody strongly diminished ErbB4 tyrosine phosphorylation, as did preincubation of the cells with MMP inhibitors SC44463, BB94 and TIMP-3 and the pro-MMP-7E219Q mutant that displays a 590-fold reduction in activity (Cha and Auld 1997; Fig. 4C). These observations support the notion that CD44HSPG may present active HB-EGF to ErbB4. Consistent with this view, addition of recombinant mature HB-EGF rescued ErbB4 tyrosine phosphorylation in CD44HSPG transfectants incubated with pro-MMP-7E219Q, but had no effect on ErbB4 tyrosine phosphorylation in CD44H and CD44v7-10 transfectants (data not shown).

MMP-7 has been proposed to promote tumor cell survival (Witty et al. 1994), and HB-EGF has been implicated in the protection of cells from apoptosis (Opanashuk et al. 1999). Consistent with these observa-

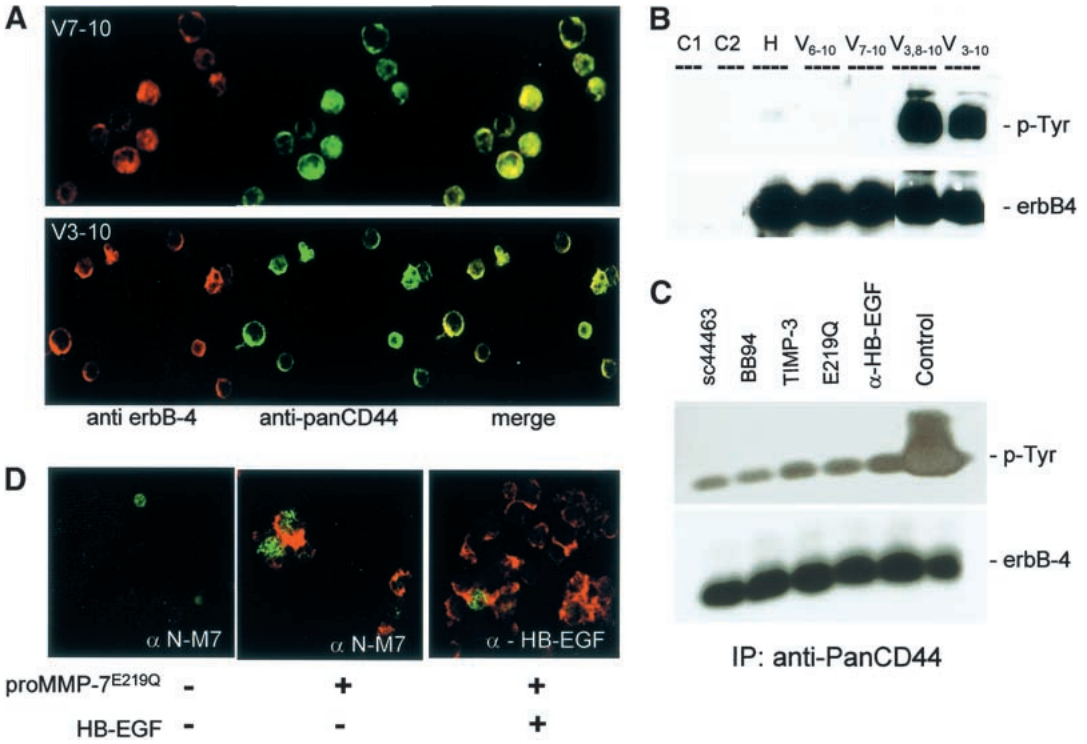

Figure 4. ErbB4 complexes with CD44 but is phosphorylated preferentially when associated with CD44v3. (*A*) Confocal microscopy shows colocalization of ErbB4 (red fluorescence) and CD44 (green fluorescence) in Namalwa CD44 transfectants. (*B*) (*Top* panel) Western blot analysis of anti-CD44 mAb immunoprecipitates from Namalwa transfectant lysates using anti-phosphotyrosine mAb pY20. (*Bottom* panel) Western blot analysis of anti-CD44 mAb immunoprecipitates in *B* immunoblotted with anti-c-ErbB4 mAb HFR-1. (*C*) HB-EGF neutralizing Ab (100 ng/mL), proMMP-7E219Q mutant (300 ng/mL), TIMP-3 (100 ng/mL), and MMP inhibitors SC44463 and BB94 (50 ng/mL) can reduce the level of tyrosine phosphorylated ErbB-4 in CD44V3-10 transfected Namalwa cells. (*Top* panel) Anti-tyrosine Ab pY20 blot. (*Bottom* panel) Anti-C-erbB-4 Ab-4 (HFR-1) blot. (*D*) Pro-MMP-7E219Q binds to the surface of Namalwa CD44HSPG and promotes apoptosis in serum-free medium. Namalwa transfectants expressing CD44v3-10 were incubated in serum free medium in the presence or absence of 100 ng/mL of recombinant proMMP-7E219Q alone or proMMP-7E219Q and recombinant active HB-EGF (50 ng/mL) as indicated. The cells were then tested for cell surface-bound MMP 7E219Q, using rat N-terminal propeptide MMP-7-specific antibody RM7-N (red fluorescence), and apoptosis, as assessed by TUNEL staining (green fluorescence). The RM7-N antibody did not react with CD44v3-10 Namalwa transfectants in the absence of exogenous rat proMMP 7E219Q (*left*). RM7-N stained CD44v3-10 Namalwa transfectants incubated with pro-MMP 7E219Q, but not CD44 transfectants lacking HSPG (data not shown). The majority of MMP-7E219Q bound cells tested TUNEL positive. Recombinant active HB-EGF (50 ng/mL) bound to the surface of transfectants preincubated with proMMP 7E219Q, as assessed by staining with neutralizing anti-HB-EGF antibody (*right*) and could rescue the majority of the cells from MMP 7E219Q binding-induced apoptosis.

tions, recombinant active MMP-7 and mature HB-EGF were each observed to rescue Namalwa CD44HSPG transfectants from serum starvation-induced cell death, whereas synthetic MMP inhibitors as well as anti-HB-EGF neutralizing antibody promoted apoptosis (data not shown). Significantly, neither recombinant MMP-7 nor HB-EGF could rescue wild type Namalwa cells and transfectants expressing non-HSPG isoforms of CD44 from serum deprivation-induced apoptosis (data not shown).

To address the role of MMP-7 in the Namalwa cell survival more selectively, we tested the effect of recombinant rat proMMP-7E219Q, which should compete with endogenous MMP-7 for binding to the surface of CD44HSPG-transfected Namalwa cells. Namalwa transfectants incubated with the recombinant mutant pro-MMP-7E219Q were stained with an antibody that specifically recognizes the prodomain of rat but not the endogenous human MMP-7 (RM7-N, Fig. 4D). Pro-MMP-7E219Q was observed to form aggregates on the surface of CD44HSPG transfectants (Fig. 4D, middle panel), but failed to bind transfectants expressing CD44 isoforms that lack the v3 exon (data not shown). Most of the cells that bound the mutant enzyme tested positive for TUNEL staining (Fig. 4D, middle panel), but could be rescued from apoptosis by the addition of recombinant active HB-EGF (Fig. 4D, right panel). Comparable results were obtained using phorbolester-stimulated neuroblastoma SH-SY5Y cells grown in soft agar (data not shown).

Postpartum uterus involution in CD44$^{-/-}$ mice is accelerated and accompanied by MMP-7 redistribution and decreased HB-EGF processing

To determine whether recruitment of MMP-7, pro-HB-EGF, and ErbB4 is a physiological function of

CD44HSPG, we explored the assembly of the complex in organs of wild-type and CD44-null DBA/1 mice that express both CD44 and MMP-7. CD44 is broadly expressed in human and mouse tissues, but CD44HSPG appears to be preferentially expressed in epithelia, including among others, postpartum uterine (W-H. Yu and I. Stamenkovic, unpubl.) and mammary gland epithelial (Roca et al. 1998) cells. MMP-7 expression has been detected in the epithelium of numerous organs, which in the mouse include the colon, kidney, lung, skin, stomach, postpartum uterus, and lactating and involuting mammary gland (Wilson et al. 1995). Because we observed DBA/1 CD44-null mice to display premature postpartum uterine and lactating mammary gland involution, we focused our attention on MMP-7/HB-EGF/ErbB4 localization and activity in these organs in wild-type and CD44$^{-/-}$ animals.

Heparan sulfate expression in the uterine epithelium varies during the estrous cycle, reaching a peak between 24 and 36 h postpartum (Yu and Woessner 2000), and closely mimics that of MMP-7 (Sellers and Woessner 1980; Wilson and Matrisian 1996; Woessner 1996). In the rat, MMP-7 proteolytic activity is present at term and its concentration rises to a peak between 24 and 36 h postpartum, which coincides with maximal glycoprotein and proteoglycan loss (Sellers and Woessner 1980). It then falls to near undetectable levels by five days postpartum. MMP-7 transcripts in the mouse uterus show a similar pattern, with the appearance of a distinct signal in the epithelium during pregnancy that reaches maximal strength between 6 and 36 h postpartum (Wilson and Matrisian 1996). Interestingly, postpartum involution of the uterus appeared to be accelerated in CD44-null DBA/l mice (Fig. 5A, a). At term, the size of the uterus in wild-type and CD44$^{-/-}$ animals was comparable (data not shown). However, 24–36 h postpartum, the size of CD44$^{-/-}$ mouse uterus was reduced to about half that of wild-type animals (Fig. 5A, a). Low power histological comparison revealed reduced wall thickness of postpartum uteri from CD44$^{-/-}$ mice, with a disorganized myometrium (Fig. 5A, b,c). At higher power, morphological changes were observed in both the epithelial (Fig. 5A, d,e) and smooth muscle layers (Fig. 5A, f,g). Lumenal epithelial cells in CD44$^{-/-}$ postpartum uteri displayed a more elongated, columnar morphology than their wild-type counterparts, with elongated nuclei (Fig. 5A, d,e). The compact disposition of wild-type myometrial smooth muscle bundles (Fig. 5A, f) was replaced by loosely coordinated, disorganized groups of smooth muscle cells with dense, slightly hyperchromatic nuclei (Fig. 5A, g).

Confocal microscopy revealed colocalization of CD44HSPG and MMP-7 on the apical surface of wild-type postpartum endometrial epithelial cells (Fig. 5B, top panel). In contrast, MMP-7 displayed a more diffuse, basal distribution in the epithelium of CD44$^{-/-}$ postpartum uteri (Fig. 5B, second panel), consistent with the possibility that CD44HSPG provides an apical cell surface-docking molecule for MMP-7. The redistribution of MMP-7 in the absence of CD44 is further illustrated by comparing anti-MMP-7 and anti-perlecan (a basement membrane proteoglycan) antibody staining of postpartum uterine epithelium in wild-type and CD44$^{-/-}$ mice. Whereas MMP-7 and perlecan localize to the apical cell surface and basement membrane, respectively, in wild-type mice (Fig. 5B, third panel), they colocalize in the basal cell compartment and in the basement membrane in CD44$^{-/-}$ mice (Fig. 5B,bottom panel).

The anti-HB-EGF neutralizing antibody that selectively recognizes the processed, mature form of HB-EGF reacted with the apical surface of uterine epithelial cells in wild-type mice, similar to the anti-MMP-7 antibody (Fig. 5C, top panel). Unlike MMP-7, pro-HB-EGF, recognized by the M-18 antibody raised against its intracellular domain, remained on the apical surface in CD44$^{-/-}$ epithelial cells (Fig. 5C, middle panel). However, the neutralizing anti-HB-EGF antibody only faintly stained the epithelial surface in CD44$^{-/-}$ animals (Fig. 5C, bottom panel), consistent with the possibility that pro-HB-EGF processing is attenuated when MMP-7 is not on the apical cell surface. Postpartum uterine smooth muscle in CD44$^{-/-}$ animals displayed similar phenotypic changes to those seen in the epithelium, with redistribution of MMP-7 to the periphery of the fibers (Fig. 5D, top and middle panels) and marked reduction in pro-HB-EGF processing (Fig. 5D, bottom panel).

The evidence that the EGF receptor family member ErbB 4 is an HB-EGF receptor (Olayioye et al. 2000; Sweeney et al. 2000) predicts that ErbB4 should display a similar tissue and cellular distribution to that of CD44HSPG and MMP-7, and that its activation, as defined by its tyrosine phosphorylation (Sweeney et al. 2000), should be detected at these sites. As expected, ErbB4 expression was observed predominantly on the apical surface of uterine epithelium and throughout the smooth muscle fibers (Fig. 5E; data not shown). Moreover, an anti-phosphotyrosine antibody reacted strongly with the apical epithelial surface of uteri from wild-type mice (Fig. 5E, top panel). In CD44$^{-/-}$ animals, ErbB4 expression was unaltered, but tyrosine phosphorylation of molecules associated with the apical epithelial cell membrane was barely detectable (Fig. 5E, bottom panel). Because of the observation that HB-EGF can protect cells from apoptosis (Opanashuk et al. 1999), postpartum wild-type and CD44$^{-/-}$ uterine tissues were compared for apoptotic cell death by TUNEL assay. Whereas there was little detectable apoptosis in the epithelium and smooth muscle of wild-type 24–48 h postpartum uteri (Fig. 5F, top and third panels), extensive apoptosis in both tissues was observed in CD44$^{-/-}$ counterparts (Fig. 5F, second and bottom panels).

Lactating mammary gland undergoes premature involution in CD44$^{-/-}$ DBA/1 mice

On average, six to eight out of 10 CD44$^{-/-}$ DBA/l mice (from a total of ⩾20 litters) were observed to die within 2 d after birth because of the impaired ability of the females to nurse. When nursed by surrogate wild-type mothers, CD44$^{-/-}$ pups develop normally, whereas 60–80% of wild-type type pups nursed by CD44$^{-/-}$ females

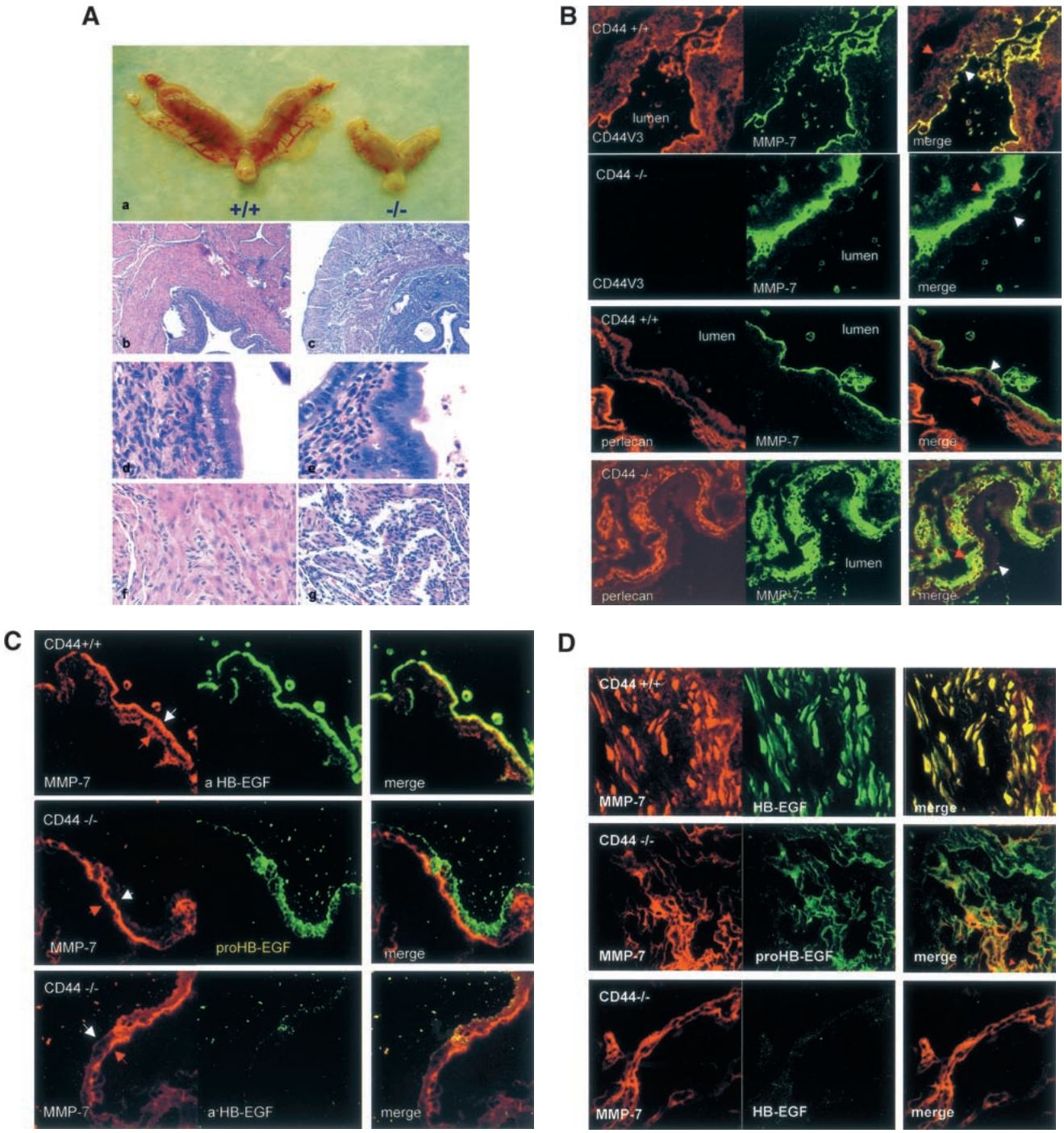

(*Figure 5 continued on facing page*)

(5–6 wild-type pups per surrogate CD44-null mother in ⩾5 experiments) die. CD44-null females do not appear to neglect their pups, and in fact bear numerous bite marks on their nipples that reflect the pups' attempts to feed (data not shown). These observations are consistent with the possibility that CD44-null mammary glands bear a developmental and/or functional defect. Mammary gland development in CD44-null mice at puberty was comparable to that in wild-type counterparts as judged by conventional histology (data not shown). However, unlike postpartum mammary glands in wild-type mice, which involute after weaning, most CD44$^{-/-}$ mouse mammary glands were found to undergo involution within 1–4 d postpartum (Fig. 6A, a; data not shown). At 2 d postpartum, mammary fat pads of wild-type females were nearly completely invested with engorged lobuloalveoli that displaced stromal adipose tissue (Fig. 6A, b,d). In contrast, mammary glands of CD44$^{-/-}$ mice displayed

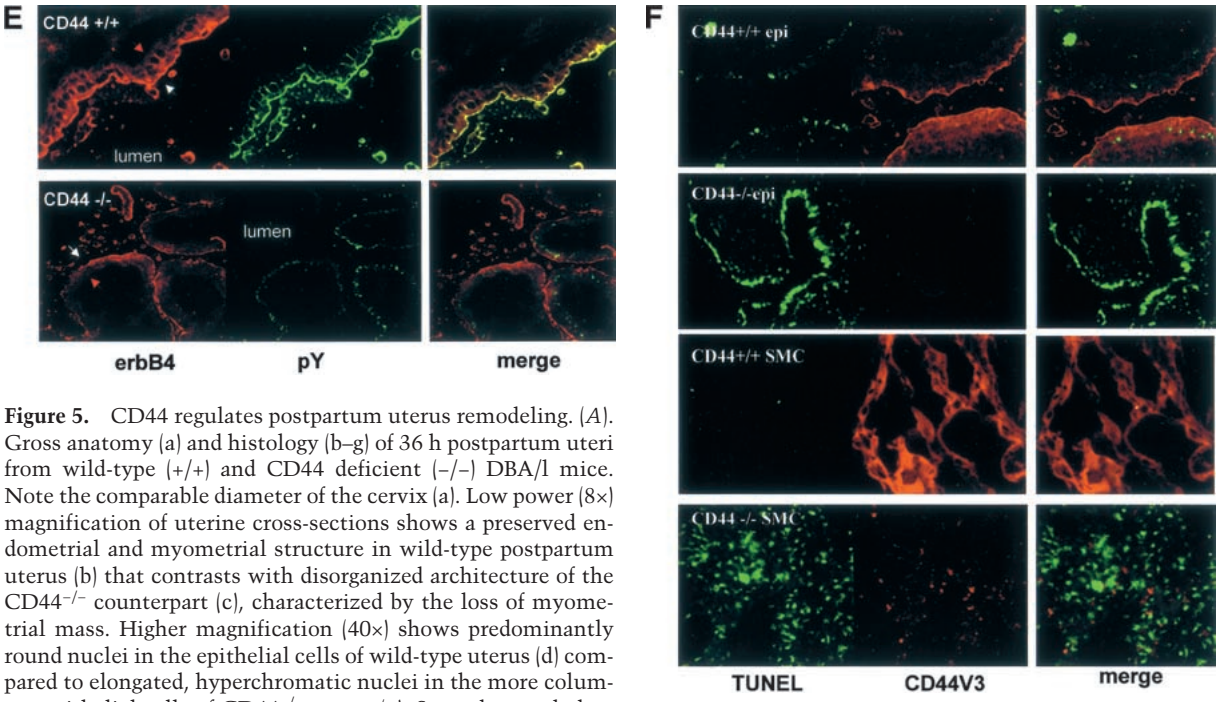

Figure 5. CD44 regulates postpartum uterus remodeling. (*A*). Gross anatomy (a) and histology (b–g) of 36 h postpartum uteri from wild-type (+/+) and CD44 deficient (–/–) DBA/1 mice. Note the comparable diameter of the cervix (a). Low power (8×) magnification of uterine cross-sections shows a preserved endometrial and myometrial structure in wild-type postpartum uterus (b) that contrasts with disorganized architecture of the CD44$^{-/-}$ counterpart (c), characterized by the loss of myometrial mass. Higher magnification (40×) shows predominantly round nuclei in the epithelial cells of wild-type uterus (d) compared to elongated, hyperchromatic nuclei in the more columnar epithelial cells of CD44$^{-/-}$ uterus (e). Smooth muscle layers are preserved in wild-type uterus (f), but appear disorganized and condensed, with hyperchromatic nuclei in CD44$^{-/-}$ uterus (g). (*B*) CD44HSPG-dependent localization of MMP-7 to the apical surface of uterine epithelium. (*Top* panels) 36 h postpartum uteri from wild-type and CD44$^{-/-}$ mice were stained with anti-CD44v3 mAb (red fluorescence) and anti-MMP-7 mAb (green fluorescence). (*Bottom* panels) Comparison of the localization of anti-MMP-7 antibody staining to that of anti-basement membrane proteoglycan perlecan antibody staining in 36 h postpartum epithelium of wild-type and CD44$^{-/-}$ mice. White and red arrows indicate the apical and basal epithelial surface, respectively. (*C*) MMP-7 and HB-EGF localization in wild-type and CD44$^{-/-}$ uterine epithelium. Thirty-six h postpartum uteri from wild-type and CD44$^{-/-}$ mice were stained with anti-MMP-7 antibody (red fluorescence) and anti-HB-EGF neutralizing antibody that recognizes the mature form only (HB-EGF), or the C-18 antibody against a peptide in the cytoplasmic tail of pro-HB-EGF (proHB-EGF, green fluorescence). White and red arrows denote the apical and basal epithelial surface, respectively. (*D*) MMP-7 and HB-EGF localization in wild-type and CD44$^{-/-}$ postpartum uterine smooth muscle. Staining was performed as in *C* and shows colocalization of MMP-7 and mature HB-EGF in wild-type smooth muscle cells (*top*). In CD44$^{-/-}$ postpartum uteri, MMP-7 is redistributed to the cell periphery, MMP-7 and pro-HB-EGF show only occasional colocalization (*middle*), and mature HB-EGF is barely detectable (*bottom*). (*E*) Colocalization of ErbB4 and phosphotyrosine in postpartum uterine epithelium. Anti-ErbB4 antibody (red fluorescence) and anti-phosphotyrosine pY20 mAb (green fluorescence) predominantly stain the apical epithelial surface in wild-type postpartum uterus (*top*). In CD44$^{-/-}$ postpartum uterus, ErbB4 distribution is unchanged, whereas apical epithelial tyrosine phosphorylation is abrogated, and only intracellular phosphorylation remains detectable. White and red arrows indicate the apical and basal epithelial surface, respectively (*F*) TUNEL (green fluorescence) and anti-CD44 mAb staining (red fluorescence) in wild-type and CD44$^{-/-}$ 48 h postpartum uteri. Wild-type (*top*) and CD44$^{-/-}$ (*second* panel) epithelial, and wild-type (*third* panel), and CD44$^{-/-}$ smooth muscle (*bottom*) staining is shown, indicating massive apoptotic cell death in both cell types in the absence of CD44.

only focal lobuloalveolar expansion (Fig. 6A, c), with many of the acini appearing condensed, and containing lumenal secretory lipids (Fig. 6A, e). Whereas wild-type mammary gland epithelium was largely negative for TUNEL staining (Fig. 6A, f), numerous TUNEL-positive cells were observed in the epithelium of CD44$^{-/-}$ mammary glands (Fig. 6A, g), consistent with extensive apoptotic cell death.

Similar to the uterine epithelium, the lobuloalveolar epithelium of lactating mammary glands displayed CD44HSPG and MMP-7 colocalization on the lumenal surface (Fig. 6B, top panel; data not shown). Similar colocalization was observed in myoepithelial cells (data not shown). In CD44$^{-/-}$ mice, MMP-7 was observed to undergo basal redistribution (Fig. 6B, second panel), as verified by comparison with perlecan localization (Fig. 6B, lower two panels). Whereas acini of wild-type mice displayed apico-lateral epithelial cell MMP-7 and basement membrane perlecan distribution (Fig. 6B, third panel), the two molecules colocalized to the basal cellular and basement membrane compartments in the acini of CD44$^{-/-}$ animals (Fig. 6B, bottom panel). Mature HB-EGF colocalized with MMP-7 in the acinar mammary gland epithelium of wild-type mice (Fig. 6C, top panel), but was only weakly visible in the acini of CD44$^{-/-}$ counterparts (Fig. 6C, middle panel), whereas pro-HB-EGF expression remained localized throughout the epithelial cells (Fig. 6C, bottom panel). Expression of ErbB4 appeared to be unaltered in CD44$^{-/-}$ mice, but tyrosine phosphorylation in the apical epithelial cell compartment (Fig. 6D, top panel) was greatly diminished (Fig. 6D, bottom panel). These alterations in MMP-7 and HB-EGF distribution, and tyrosine phosphorylation associated with the apical epithelial cell membrane are similar

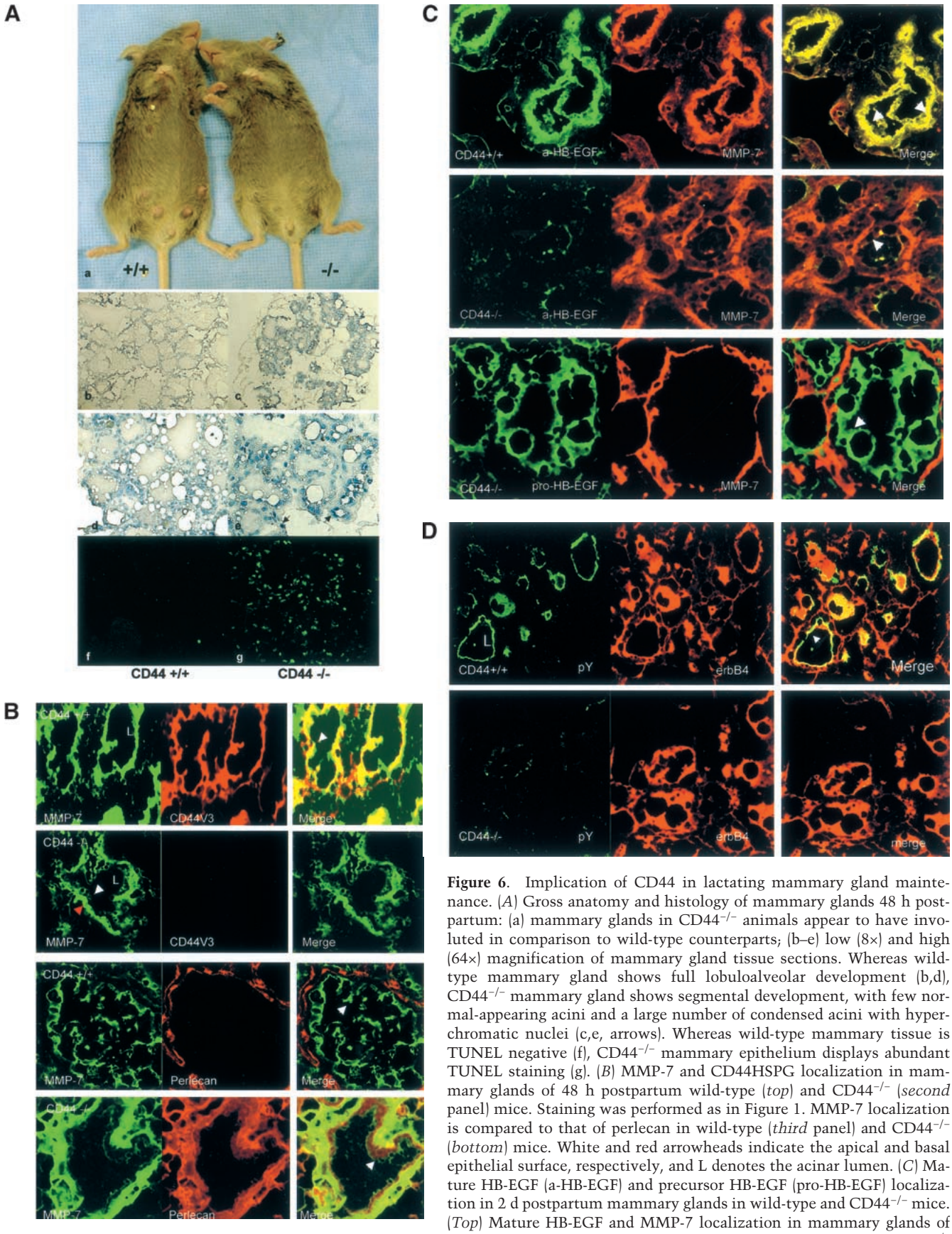

Figure 6. Implication of CD44 in lactating mammary gland maintenance. (*A*) Gross anatomy and histology of mammary glands 48 h postpartum: (a) mammary glands in CD44$^{-/-}$ animals appear to have involuted in comparison to wild-type counterparts; (b–e) low (8×) and high (64×) magnification of mammary gland tissue sections. Whereas wild-type mammary gland shows full lobuloalveolar development (b,d), CD44$^{-/-}$ mammary gland shows segmental development, with few normal-appearing acini and a large number of condensed acini with hyperchromatic nuclei (c,e, arrows). Whereas wild-type mammary tissue is TUNEL negative (f), CD44$^{-/-}$ mammary epithelium displays abundant TUNEL staining (g). (*B*) MMP-7 and CD44HSPG localization in mammary glands of 48 h postpartum wild-type (*top*) and CD44$^{-/-}$ (*second* panel) mice. Staining was performed as in Figure 1. MMP-7 localization is compared to that of perlecan in wild-type (*third* panel) and CD44$^{-/-}$ (*bottom*) mice. White and red arrowheads indicate the apical and basal epithelial surface, respectively, and L denotes the acinar lumen. (*C*) Mature HB-EGF (a-HB-EGF) and precursor HB-EGF (pro-HB-EGF) localization in 2 d postpartum mammary glands in wild-type and CD44$^{-/-}$ mice. (*Top*) Mature HB-EGF and MMP-7 localization in mammary glands of wild-type mice. (*Middle* and *bottom*) Mature and pro-HB-EGF localization in comparison to MMP-7 in mammary glands of CD44$^{-/-}$ mice. White arrows indicate the lumenal epithelial surface. (*D*) Localization of phosphotyrosine (pY) and ErbB4 in wild-type and CD44$^{-/-}$ mammary epithelium. Tyrosine phosphorylation is greatly reduced in CD44$^{-/-}$ epithelium whereas ErbB4 expression is unaltered.

to those observed in the epithelium and smooth muscle of postpartum uterus.

MMP-7 has been proposed to be weakly expressed in lactating and involuting mouse mammary gland, detectable only by RT–PCR (Wilson et al. 1995). Our results, however, suggest relatively abundant expression. This discrepancy may be attributable, in part, to the different detection methods used, one study analyzing transcript and the other protein expression using a sensitive antibody. It is conceivable that differences in protein and corresponding transcript stability might account, at least in part, for higher protein expression than might be predicted by mRNA levels. Differences in mouse strains (lCR mice in the study by Wilson et al., and DBA/1 mice in the present work) may also underlie expression level variation.

Pro-HB-EGF processing and ErbB4 tyrosine phosphorylation are reduced in CD44$^{-/-}$ postpartum uteri and lactating mammary glands

To provide further evidence that pro-HB-EGF processing is reduced in postpartum uteri and lactating mammary glands of CD44$^{-/-}$ mice, and to verify that the reduction of tyrosine phosphorylation observed on tissue sections is attributable, at least in part to that of ErbB4, we assessed pro-HB-EGF expression and ErbB4 tyrosine phosphorylation in the relevant tissues. Western blot analysis of HB-EGF expression was performed on lysates of wild-type and CD44$^{-/-}$ 24–36 h postpartum uteri and lactating mammary glands, using a combination of the M-18 antibody that recognizes pro-HB-EGF and neutralizing anti-HB-EGF antibody that recognizes processed HB-EGF only. Immunoprecipitation studies have shown that HB-EGF precursor can be expressed as several species ranging between 22 and 30 kD that vary among cell types, possibly due to posttranslational modifications (Suzuki et al. 1997; Opanashuk et al. 1999; Prenzel et al. 1999; Gechtman et al. 2000). Processed, mature forms display a molecular weight range of 14–19 kD (Opanashuk et al. 1999; Prenzel et al. 1999; Gechtman et al. 2000). Using the combination of M-18 and neutralizing anti-HB-EGF antibodies, which allows recognition of both precursor and processed HB-EGF, we observed a comparable band pattern on uterine and mammary tissue Western blots (Fig. 7A). Moreover, whereas wild-type tissues contained several HB-EGF species, ranging from 12–28 kD, consistent with both processed and precursor forms (Opanashuk et al. 1999; Gechtman et al. 2000), CD44$^{-/-}$ tissues predominantly displayed the 27–28 kD species characteristic of pro-HB-EGF (Fig. 7A). Western blot analysis, using anti-phosphotyrosine antibody pY20, of ErbB4 immunoprecipitates from wild-type and CD44$^{-/-}$ postpartum uterine and lactating mammary gland homogenates, revealed a strong reduction in tyrosine phosphorylation of ErbB4 derived from CD44$^{-/-}$ tissues (Fig. 7B).

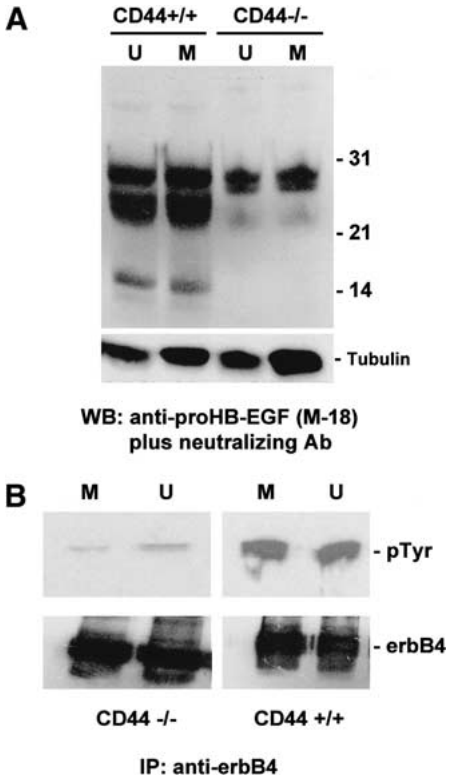

Figure 7. HB-EGF processing and ErbB4 tyrosine phosphorylation in 48 h postpartum uteri and lactating mammary glands of wild-type and CD44$^{-/-}$ mice. (*A*) 48 h postpartum uterine (U) and lactating mammary gland (M) lysates (~80 µg of lysate per lane) from the indicated animals were tested for HB-EGF expression by Western blot analysis using a combination of anti-pro-HB-EGF C-18 and neutralizing anti-HB-EGF antibodies. Anti-tubulin antibody (*bottom*) was used as a loading control. (*B*) Western blot analysis (*top*) of anti-ErbB4 antibody immunoprecipitates (*bottom*) from 48 h postpartum uteri (U) and lactating mammary glands (M) using anti-pY20 antibody.

Discussion

In the present work, we have uncovered two possibly related functions of CD44. The first is the assembly by CD44HSPG of a cell surface complex composed of MMP-7, pro-HB-EGF, and ErbB4. The second is participation in the regulation of postpartum uterine and lactating mammary gland involution. Assembly of the MMP-7/HB-EGF/ErbB4 complex, and appropriate localization of MMP-7 proteolytic activity to the epithelial and smooth muscle cell surface may provide at least part of the mechanism whereby CD44 regulates female reproductive organ remodeling.

CD44HSPG-dependent cell surface localization of MMP-7 and complex assembly

Evidence from both in vivo and in vitro studies, suggests that CD44HSPG plays a central role in the assembly of the MMP-7/HB-EGF/ErbB4 complex in the appropriate cellular location. In the absence of CD44HSPG, MMP-7 was observed to undergo redistribution in postpartum uterine endometrial cells as well as in lactating mammary epithelial cells from the apical to the basal compartment. One possible explanation for this relocaliza-

tion is that in the absence of CD44HSPHG, MMP-7 binds to alternative HSPG docking sites that are predominantly expressed on the basal surface of epithelial cells and in the basement membrane. Redistribution of MMP-7 was accompanied by decreased pro-HB-EGF processing, as illustrated by the reduction of mature but not pro-HB-EGF expression in the epithelium, and inhibition of ErbB4 tyrosine phosphorylation. Similar observations were made in uterine smooth muscle, suggesting that in the absence of CD44, the MMP-7/HB-EGF/ErbB4 complex cannot be assembled in the mouse postpartum uterus and lactating mammary gland.

The ability of CD44HSPG, but not other CD44 isoforms, to reconstitute a functional MMP-7/HB-EGF/ErbB4 complex in CD44-negative lymphoma cells, not only supports the notion that CD44HSPG coordinates MMP-7 and HB-EGF association in vivo, but, consistent with previous studies (Bennett et al. 1995; Yu and Woessner 2000), underscores the requirement for heparan sulfate for the recruitment of both molecules. It also suggests that the ability of CD44HSPG to assemble the complex is a general phenomenon that is likely to be observed in most cells that express the constituent molecules. A hypothetical representation of the assembly and function of the CD44HSPG/MMP-7/HB-EGF/ErbB4 complex is shown in Figure 8. In this model, MMP-7 and pro-HB-EGF are recruited to the cell surface by the HS chains of CD44HSPG. MMP-7 proteolytically processes pro-HB-EGF, and mature HB-EGF is presented by the CD44-associated HS to ErbB4, which is connected to CD44 by a hypothetical intracellular adaptor protein. Engagement by HB-EGF induces tyrosine phosphorylation of ErbB4 and the transduction of signals that can trigger proliferation, differentiation, and survival.

MMP-7-mediated HB-EGF processing and cell survival

Pro-HB-EGF is expressed as an integral membrane protein of 22–28 kD, depending, in part, on posttranslational modification (Higashiyama et al. 1992, 1993; Gechtman et al. 2000). Stimulation of pro-HB-EGF-producing cells with phorbolester and other mitogens results in the release of mature soluble 14–19 kD HB-EGF polypeptides that function in autocrine or paracrine fashion (Opanashuk et al. 1999; Prenzel et al. 1999; Gechtman et al. 2000). Postpartum uterine and lactating mammary gland lysates from wild-type mice in the present study, revealed the presence of several HB-EGF species, ranging from 12–28 kD, consistent with those released from phorbolester-stimulated tumor cells (Gechtman et al. 2000) and kinaic acid-stimulated neurons (Opanashuk et al. 1999). In contrast, the corresponding lysates from $CD44^{-/-}$ animals predominantly displayed 27–28 kD species that are consistent with pro-HB-EGF. These observations provide biochemical evidence that in the absence of the CD44HSPG-assembled complex, pro-HB-EGF processing is reduced in the uterus and mammary gland. Incubation of CD44HSPG-associated pro-HB-EGF with recombinant active MMP-7 resulted in the generation of 8–19 kD peptides consistent with the reported mature species (Opanashuk et al. 1999; Prenzel et al. 1999; Gechtman et al. 2000). CD44HSPG-associated pro-HB-EGF processing was not observed in the presence of EDTA, which removes endogenous MMPs, and occurred only when exogenous recombinant active MMP-7 was added. These observations indicate that pro-HB-EGF is a substrate of MMP-7.

Thus far, at least two candidate proteolytic enzymes have been proposed to process pro-HB-EGF. One is ADAM 9 (Izumi et al. 1998), although this claim is disputed (Prenzel et al. 1999). The other is MMP-3 (Suzuki et al. 1997). The relative contribution of MMP-3 and MMP-7 to pro-HB-EGF processing remains to be determined. The coexpression of MMP-7 and HB-EGF in the uterus and mammary gland, and their shared affinity for HSPG, suggest that MMP-7 may provide a major processing mechanism for pro-HB-EGF in these tissues. Consis-

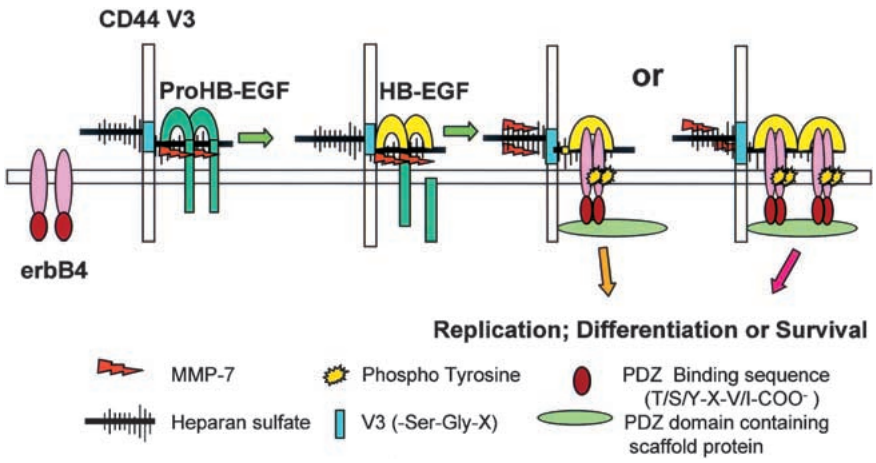

Figure 8. Hypothetical assembly and function of the CD44HSPG/MMP 7/HB-EGF/ErbB4 complex. CD44HSPG isoforms bind proHB-EGF and active MMP-7. MMP-7 proteolytically cleaves proHB-EGF, generating mature HB-EGF, which is presented by CD44HSPG to ErbB4. Engagement of ErbB4 by HB-EGF results in tyrosine phosphorylation of its intracellular domain and the transduction of signals that promote survival. ErbB4 may be induced to form homodimers or multimers. Indirect intracellular domain-mediated interaction between CD44 and ErbB4 is proposed, based on the presence of PDZ binding motifs in the intracellular domain of both CD44 (Stamenkovic et al. 1991) and ErbB4 (Garcia et al. 1999), which may bind a common scaffold protein. The mechanism of interaction between CD44 and ErbB family members is presently unknown and the representation is purely speculative.

tent with this view, MMP-3 expression displayed a predominantly stromal distribution in the uterus and mammary gland in wild-type mice, and was absent in Namalwa cells (data not shown). However, this neither invalidates the role of MMP-3 as a pro-HB-EGF processor, nor does it exclude the possibility that MMP-3 may play a more dominant role in other situations, such as stromal remodeling in inflammation and repair.

HB-EGF has been proposed to protect cells from apoptosis (Opanashuk et al. 1999). However, in addition to processing pro-HB-EGF, MMP-7 has been shown to cleave FasL (Powell et al. 1999), whose effectiveness in triggering Fas-mediated tumor cell death is reduced in soluble form (Schneider et al. 1998). MMP-7 may therefore protect cells from apoptosis by more than one mechanism. The Namalwa cells used in the present study do not express Fas, and the observations that recombinant active MMP-7 and mature HB-EGF can each rescue Namalwa CD44HSPG transfectants from serum starvation-induced apoptosis, suggest that processing of pro-HB-EGF in the context of CD44HSPG provides a plausible mechanism whereby MMP-7 promotes cell survival.

The possible role of the CD44HSPG/MMP-7/HB-EGF/ErbB4 complex in postpartum uterine and lactating mammary gland involution

Postpartum uterine involution in $CD44^{-/-}$ animals was observed to be accelerated in comparison to that in normal counterparts, and was accompanied by extensive epithelial and smooth muscle cell apoptosis. Similarly, most lactating mammary glands in these animals were characterized by varying degrees of lobuloalveolar condensation with only focal acinar expansion, suggesting that the lactating phenotype in DBA/1 mice cannot be fully sustained in the absence of CD44. Because CD44 fulfills multiple functions, including that of a cell surface hyaluronan receptor, any attribution of the regulation of female reproductive organ remodeling to a single function of CD44 must be made with caution. Nevertheless, it is tempting to speculate that the premature postpartum uterine and lactating mammary gland involution observed in CD44-null mice is related to the disruption of the CD44HSPG-dependent complex. To provide a plausible suggestion for such a relationship, the observation that MMP-7 null mice do not display aberrant remodeling of either organ (Rudolph-Owen et al. 1997) must be taken into account. The premature reproductive organ involution displayed by $CD44^{-/-}$ mice may therefore be related not to the loss of MMP-7 activity, but rather to its mislocalization. Redistribution of MMP-7 to the basal compartment of $CD44^{-/-}$ epithelial cells, whether in the uterus or mammary gland, may have at least two consequences. The first is impaired pro-HB-EGF processing on the epithelial cell surface resulting in the reduction of ErbB4 activation and generation of the corresponding survival signals. The second is inappropriate concentration of MMP-7 proteolytic activity on the basal surface of epithelial cells, and in the basement membrane, leading to basement membrane degradation and potential activation of other locally sequestered MMPs. ECM degradation is believed to provide the principal mechanism for postpartum uterine contraction. Consistent with this notion, the ability of MMP-7 to hydrolyze a broad range of ECM substrates (Rudolph-Owen et al. 1997), renders likely the possibility that its mislocalization in, or inappropriate release from, epithelial and smooth muscle cells lacking CD44HSPG augments ECM degradation and accelerates the involution process. Thus, at the very least, CD44HSPG-mediated docking of MMP-7 may help control physiological reproductive tissue remodeling and prevent inappropriate ECM degradation.

It is noteworthy that MMP-7 null mice do not display premature lactating mammary gland involution (Rudolph-Owen et al. 1997), which might be expected if HB-EGF provides an essential lactating mammary epithelial cell survival signal and if processing of its precursor is under the exclusive control of MMP-7. However, loss of MMP-7 expression is accompanied by a several fold increase in the expression of other MMPs, including MMP-3 (Rudolph-Owen et al. 1997), which processes proHB-EGF. It is therefore conceivable that MMP-3, or possibly other metalloproteinases, compensate for the loss of MMP-7-mediated proHB-EGF processing in these mice.

Recent work by others provides support for the notion that the CD44HSPG/MMP-7/HB-EGF/ErbB4 complex may participate in maintaining the lactating mammary gland phenotype. MMP-7 is expressed in the epithelium of exocrine glands and its broad substrate specificity has been proposed to help regulate exocrine duct patency (Saarialho-Kere et al. 1995). ErbB4 is also expressed in mammary gland epithelium, and appears to play a prominent role in mammary gland differentiation and maintenance (Jones et al. 1999). Although highly expressed throughout pregnancy, ErbB4 tyrosine phosphorylation is first detected in late pregnancy, when epithelial differentiation and secretory activity predominate over proliferation, and peaks during lactation when mammary epithelium undergoes terminal differentiation (Jones et al. 1999). Expression of a dominant negative ErbB4 was observed to result in premature lobuloalveolar condensation in midlactation (Jones et al. 1999). The mammary gland phenotype in transgenic mice expressing a dominant negative ErbB4 is reminiscent of that observed in the $CD44^{-/-}$ animals in the present study, although it appears only in midlactation. The earlier appearance of lobuloalveolar condensation in $CD44^{-/-}$ animals may reflect increased proteolytic degradation of ECM by mislocalized MMP-7, or possibly, the loss of a CD44 function that is unrelated to the complex. However, our observations, combined with the notion that HB-EGF promotes cell survival in other situations (Opanashuk et al. 1999), are consistent with the possibility that ErbB4 engagement by mature HB-EGF may be implicated in protecting epithelial cells from apoptosis during tissue remodeling. Integrin-mediated epithelial survival signals, generated by engagement of

basement membrane ligands, may be impaired as a result of ECM disruption that accompanies tissue remodeling, and epithelial cells may temporarily require alternative signals to ensure protection from anoikis (Frisch and Ruoslahti 1997). One conceivable function of the complex assembled by CD44HSPG may be to generate such signals.

The present study supports the emerging view that cell surface docking of secreted MMPs by adhesion receptors may regulate not only ECM degradation, but growth factor activity as well (Brooks et al. 1996; Chen 1996; Murphy and Gavrilovic 1999; Bergers and Coussens 2000; Yu and Stamenkovic 2000), and suggests that localization may play a critical role in determining the effect of MMP proteolytic activity on pathophysiological processes. Our observations have also helped highlight two hitherto unrecognized physiological functions of CD44. The first is the ability of CD44HSPG to provide a unique scaffold for the recruitment and functional coordination of molecules that may play an important role in tissue remodeling and maintenance. The second is participation in the regulation of female reproductive organ remodeling. Although these two functions may well be related, further work will be required to determine the degree to which the CD44HSPG-assembled complex is implicated in the control of postpartum uterine involution and lactating mammary gland phenotype.

Materials and methods

Generation of CD44-deficient mice

The gene-targeting vector was constructed to delete sequences within exons 4 and 5 of the murine CD44 gene that code for the hyaluronan binding site (Peach et al. 1993). The murine DBA/l lacJ genomic sequences used to produce the CD44 targeting vector were amplified using long template PCR (Boerhinger-Mannheim) with primers derived from the murine CD44 cDNA sequences (Wolffe et al. 1994). The amplified genomic fragments were subcloned and the sequence confirmed. The CD44 gene was targeted in DBA/l lacJ ES cells as described previously (Roach et al. 1995), and DBA/l ES cells with the preplanned CD44 mutation were identified by Southern analysis. Chimeric offspring were produced after microinjection of DBA/l ES cells into C57/Bl6 blastocysts. Germ-line transmission of the targeted ES cells and identification of $CD44^{-/-}$ offspring on the inbred DBA/l background has been described previously (Roach et al. 1995).

Tissue specimens

Samples of female wild-type and $CD44^{-/-}$ DBA/1 mouse uterus and mammary gland at various time points postpartum were rapidly dissected, washed with cold PBS, embedded in OCT, frozen in an isobutanol bath in liquid nitrogen, and stored at –80°C until further processing. Sections 5 µm thick were cut in a cryostat, mounted onto slides, air-dried at 4°C, and rinsed twice with 90% ethanol followed by PBS to remove the OCT. The sections were then fixed in 100% methanol for 20 min, washed in PBS, and subjected to antibody staining.

Tissue staining and confocal microscopy

Tissue sections were blocked with PBS/10% serum (Jackson Laboratory) derived from the same animal species as the secondary antibody used, at room temperature for 40 min prior to incubation with the primary antibodies. Primary antibodies included: polyclonal rabbit anti-MMP-7 antibody RM7-C and polyclonal rabbit anti-MMP-7 antibody RM7-N for rat proMMP-7 (Yu and Woessner 2000); anti-panCD44 mAb clone 241, and anti-CD44V3 mAb (R&D Systems); anti-pro-HB-EGF C-18 antibody (Santa Cruz Biotechnology) for human samples and anti-pro-HB-EGF M-18 antibody (Santa Cruz) for mouse samples; anti-HB-EGF neutralizing antibody (R&D Systems); monoclonal anti-ErbB4 Ab-4 (HFR-1), polyclonal rabbit anti-ErbB4 Ab-2 (NeoMarkers), rat anti-human and mouse perlecan antibody (Chemi-Con). Incubation with primary antibodies was performed overnight at 4°C. The sections were then washed in PBS, incubated with secondary fluorescein- or Texas Red-conjugated polyclonal anti-rabbit IgG or anti-mouse IgM or IgG (Jackson Immunoresearch Laboratories) at room temperature for 45 min, washed, and analyzed by confocal microscopy (inverted Zeiss LSM 510). Images were captured at 0.6 nm increments along the *z* axis and converted to composite images by ImageSpace 3.10 software (Molecular Dynamics). Staining of cells was performed prior to (surface staining) or following (intracellular staining) fixation in 4% paraformaldehyde for 10 min at room temperature. Cells were then mounted onto cover slips and examined by confocal microscopy.

Expression constructs

The cDNA constructs used in these experiments were derived from those described previously (Stamenkovic et al. 1991; Bennett et al. 1995; unpublished reagents). All of the CD44 cDNAs, including CD44H, CD44v6-10, CD44v7-10, CD44v3, 8-10 and CD44v3-10 were subcloned into the pcDNA6His-v5 expression vector (Invitrogen). Human MMP-7 cDNA was amplified from a human colorectal carcinoma HT29 cell line cDNA expression library by PCR using synthetic oligonucleotide primers complementary to the 5′ and 3′ extremities of the coding sequence. The amplicons were inserted into pEF6V5Hisvectors (Invitrogen). *E. coli*-derived recombinant human active MMP-7 was expressed in BL21(DE3) cells using the PET3a vector (Yu and Woessner 2000) and recombinant pro-MMP-7 containing the E219Q mutation was prepared by site-directed mutagenesis, as described previously (Yu and Woessner 2000). Recombinant MMP-7E219Q lacking the propeptide, prepared in *E. coli*, was a gift from Dr. David Auld. Full-length TIMP-3 was prepared from the conditioned medium of TIMP-3 PUNT-BHK cells.

Cell lines and cell culture

SH-SY5Y and Namalwa cells were maintained in RPMI medium and CHO cells in DMEM, supplemented with 10% heat-inactivated fetal bovine serum (FBS, Irvine Scientific) and 1% penicillin and streptomycin. Namalwa cells were transfected with CD44 constructs by electroporation (400V, 960 uF), and transfectants were selected for resistance to G418 (GIBCO BRL) at a concentration of 1.0 mg/mL.

Substrate zymography

Bovine carboxy-methylated-transferrin substrate was prepared as described (Yu and Woessner 2000). Pig gelatin type A (Sigma, 0.5 mg/mL) was embedded in 7.5% SDS–polyacrylamide gels and CM-transferrin (0.3 mg/mL) in 12.5% gels. Samples were subjected to electrophoresis. Gels were washed with buffer containing 2.5% Triton X-100, 50 mM Tris (pH 7.5) at 4°C to remove SDS, and then with buffer supplemented with 5 mM $CaCl_2$. Gels were then washed with incubation buffer (50 mM

Tris at pH 7.5, 5 mM $CaCl_2$) and incubated in the same buffer with protease inhibitors (50 mM each of ZPCK, TPCK, TLCK, and 4-(2-aminoethyl)-benzenesulfonyl chloride (Calbiochem) for 18 h at 37°C. Gels were stained with 0.1% Coomassie Blue in 40% MeOH, 10% acetic acid for 45 min, and destained with 7% acetic acid.

Tissue extracts

Samples (uteri and mammary glands) were collected 24–48 h postpartum, washed with cold Ca^{++}/Mg^{++}-containing PBS, minced, and polytron-homogenized in lysis buffer (see below) at 4°C. Homogenates were spun in a microfuge for 10 min, and the soluble fraction was extracted, and subjected to immunoprecipitation with appropriate antibodies.

Immunoprecipitation and Western blot analysis

Immunoprecipitation and Western blot analysis were performed according to standard procedures. Coimmunoprecipitation of cell surface molecules was performed following preincubation of the cells with the block solution containing 4% goat serum, 50 µM zinc chloride, and protease inhibitors ZPCK, PMSF, AEBSF, leupeptin, and phosphoramadon in PBS. Cells were then incubated with the primary antibodies overnight at 4°C, in the same blocking solution, washed extensively with PBS in the presence of 50 µM zinc chloride, and lysed with a lysis buffer containing 1.25% Triton X-100 50 mM Tris (pH 7.5), 0.15 M NaCl, 10 mM $CaCl_2$, 5 mM $MgCl_2$, 50 µM $ZnCl_2$, and 50 µM each of ZPCK, TPCK, TLCK, and 500 µM 4-(2-aminoethyl)-benzenesulfonyl chloride (Calbiochem) and 1 µg/mL each of aprotinin, leupeptin, and pepstatin (Sigma Co.). Lysates were cleared for 15 min by centrifugation at 16,000 g at 4°C. Cell surface complexes were immunoprecipitated by incubation with Protein A+G agarose (Pierce Chemical Co.) beads at room temperature for 45 min followed by centrifugation. Following washes with 0.25% Triton X-100 50 mM Tris (pH 7.5), 0.15 M NaCl, 10 mM $CaCl_2$, 5 mM $MgCl_2$, 50 µM $ZnCl_2$ (Buffer W), the samples were loaded in nonreducing SDS sample buffer, subjected to electrophoresis, and transblotted onto 0.45 µm pore-size nitrocellulose membrane. Antibodies used for Western blot analysis of CD44, MMP-7, HB-EGF, and ErbB4 were anti-pan CD44 clone 241 (Human), anti MMP-7 C-RM7, anti-pro-HB-EGF (C-18), and anti erb-B4 Ab-4 HFR-1 (NeoMarkers), respectively. For HB-EGF, an additional mAb that recognizes only the fully processed, active form of HB-EGF and neutralizes its activity (R&D systems) was used in Western blot experiments. For tubulin recognition, anti-tubulin antibody 4 (NeoMarkers) was used. Immunoprecipitation of ErbB4 was performed using ErbB4 Ab-1 (NeoMarkers).

Pro-HB-EGF proteolytic cleavage with E. coli*-derived purified active MMP-7*

After performing coimmunoprecipitation of CD44 and proHB-EGF using, anti-panCD44 clone 241 mAb, the immunoprecipitated complex was washed in a PBS buffer containing 25 mM EDTA to deplete the endogenous MMP-7 from the complex, followed by several washes with 0.25% Triton X-100 50 mM Tris (pH 7.5), 0.15 M NaCl, 10 mM $CaCl_2$, 5 mM $MgCl_2$. Next ~50 ng/mL of *E. coli*-derived purified active human MMP-7 was added to the complex and incubated at 37°C overnight in the presence or absence of MMP inhibitors SC44463 or BB94, followed by Western blot analysis by using a mixture of anti-pro-HB-EGF (C-18) antibody and anti-HB-EGF neutralizing mAb.

Apoptosis assays

Tunnel assays were performed on tissue sections and cells in culture using the In Situ Cell Death Detection Kit (Boehringer Mannheim) according to the manufacturer's recommendations. After 24 h culturing the cells in serum-free medium, Namalwa transfectants were incubated without additional reagents or with recombinant HB-EGF at 50 ng/mL, anti-HB-EGF neutralizing mAb 100 ng/mL, recombinant active MMP-7 at 100 ng/mL, and recombinant proMMP-7E219Q at 300 ng/mL. The cells were incubated in serum free culture medium supplemented or not with the above reagents for another 24 h and assessed for TUNEL positive staining by fluorescence microscopy.

Acknowledgments

We thank David Auld for the recombinant processed MMP-7E219Q, Shuan-Su Yu for technical help, and Daniel Haber for critical review of the manuscript and comments. This work was supported by NIH grants CA55735 and GM48614 to I.S.

The publication costs of this article were defrayed in part by payment of page charges. This article must therefore be hereby marked "advertisement" in accordance with 18 USC section 1734 solely to indicate this fact.

References

Abramson, S.R. and Woessner, J.F.1994. Characterization of rat matrilysin and its cDNA. *Ann. New York Acad. Sci.* **232:** 362–364.

Aruffo, A., Stamenkovic, I., Melnick, M., Underhill, C.B., and Seed, B. 1990. CD44 is the principal cell surface receptor for hyaluronate. *Cell* **61:** 1303–1313.

Bartolazzi, A., Jackson, D., Bennett, K., Aruffo, A., Dickinson, R., Shields, J., Whittle, N., and Stamenkovic, I. 1995. Regulation of growth and dissemination of human lymphoma by CD44 splice variants. *J. Cell Sci.* **108:** 1723–1733.

Bennett, K.L., Jackson, D.G., Simon, J.C., Tanczos, E., Peach, R., Modrell, B., Stamenkovic, I., Plowman, G., and Aruffo, A. 1995. CD44 isoforms containing exon V3 are responsible for the presentation of heparin-binding growth factor. *J. Cell Biol.* **128:** 687–698.

Bergers, G. and Coussens, L.M. 2000. Extrinsic regulators of epithelial tumor progression: Metalloproteinases. *Curr. Opin. Genet. and Dev.* **10:** 120–127.

Bode, W., Grams, F., Reinemer, P., Gomis-Ruth, F.X., Baumann, U., McKay, D.B., and Stocker, W. 1996. The metzincin-superfamily of zinc-peptidases. *Adv. Exp. Med. Biol.* **389:** 1–11.

Brooks, P.C., Strömblad, S., Sanders, L.C., von Schalscha, T.K., Aimes, T.L., Stetler-Stevenson, W.G., Quigley, J.P., and Cheresh, D.A. 1996. Localization of matrix metalloproteinase MMP-2 to the surface of invasive cells by interaction with integrin αv β3. *Cell* **85:** 683–693.

Butler, T.A., Zhu, C., Mueller, R.A., Fuller, G.C., Lemaire, W.J. and Woessner, J.F. 1991. Inhibition of ovulation in the perfused rat ovary by the synthetic collagenase inhibitor SC 44463. *Biol. Reprod.* **44:** 1183–1188.

Cha, J. and Auld, D.S. 1997. Site-directed mutagenesis of the active site glutamate of human matrilysin: Investigation of its role in catalysis. *Biochemistry* **36:** 16019–16024.

Chen, W-T. 1996. Proteases associated with invadopodia, and their role in degradation of extracellular matrix. *Enzyme Protein* **49:** 59–71.

Frisch, S.M. and Ruoslahti, E. 1997. Integrins and anoikis. *Curr. Opin. Cell Biol.* **9:** 701–706.

Garcia, R.A.G., Vasudevan, K., and Buonanno, A. 1999. The neuregulin receptor ErbB4 interacts with PDZ-containing proteins at neuronal synapses. *Proc. Natl. Acad. Sci.* **97:** 3596–3601.

Gechtman, Z., Alonso, J.L., Raab, G., Ingber, D.E., and Klagsbrun, M. 2000. The shedding of membrane-anchored heparin-binding epidermal-like growth factor is regulated by the Raf/mitogen-activated protein kinase cascade and by cell adhesion and spreading. *J. Biol. Chem.* **274:** 28828–28835.

Higashiyama, S., Lau, K., Besner, G.E., Abraham, J.A., and Klagsbrun, M. 1992. Structure of heparin-binding EGF-like growth factor. *J. Biol. Chem.* **276:** 6205–6212.

Higashiyama, S., Abraham, J.A., and Klagsbrun, M. 1993. Heparin-binding EGF-like growth factor stimulation of smooth muscle cell migration: Dependence on interactions with cell surface heparan sulfate. *J. Cell Biol.* **122:** 933–940.

Izumi, Y., Hirata, M., Hasuwa, H., Iwamoto, R., Umata, T., Miyado, K., Tamai, Y., Kurisaki, T., Sehara-Fujisawa, A., Ohno, S., and Mekada, E. 1998. A metalloproteinase-disintegrin MDC9/meltrin-γ/ADAM 9 and PKCδ are involved in TPA-induced ectodomain shedding of membrane-anchored heparin binding-EGF-like growth factor. *EMBO J.* **17:** 7260–7272.

Jones, F.E., Welte, T., Fu, X-Y., and Stern, D.F. 1999. ErbB4 signaling in the mammary gland is required for lobuloalveolar development and Stat5 activation during lactation. *J. Cell Biol.* **147:** 77–87.

Kaya, G., Rodriguez, I., Jorcano, L., Vassalli, P., and Stamenkovic, I. 1997. Selective suppression of CD44 in keratinocytes of mice bearing an antisense CD44 transgene driven by a tissue-specific promoter disrupts hyaluronate metabolism in the skin and impairs keratinocyte proliferation. *Genes & Dev.* **11:** 996–1007.

Lesley, J., Hyman, R., and Kincade, P.W. 1993. CD44 and its interaction with extracellular matrix. *Adv. Immunol.* **54:** 271–335.

Lukashev, M.E. and Werb, Z. 1998. ECM signaling: Orchestrating cell behavior and misbehavior. *Trends Cell Biol.* **8:** 437–441.

Marikovsky, M., Breuing, K., Liu, P.Y., Eriksson, E., Higashiyama, S., Farber, P., Abraham, J., and Klagsbrun, M. 1993. Appearance of heparin-binding EGF-like growth factor in wound fluid as a response to injury. *Proc. Natl. Acad. Sci.* **90:** 3889–3893.

Murphy, G. and Gavrilovic, J. 1999. Proteolysis and cell migration: Creating a path? *Curr. Opin. Cell Biol.* **11:** 614–621.

Nagase, H. and Woessner, J.F. 1999. Matrix metalloproteinases. *J. Biol. Chem.* **274:** 21491–21494.

Olayioye, M.A., Neve, R.M., Lane, H.A., and Hynes, N.E. 2000. The ErbB signaling network: Receptor heterodimerization in development and cancer. *EMBO J.* **19:** 3159–3167.

Opanashuk, L.A., Mark, R.J., Porter, J., Damm, D., Mattson, M.P., and Seroogy, K.B. 1999. Heparin-binding epidermal growth factor-like growth factor in hippocampus: Modulation of expression by seizures and anti-excitotoxic action. *J. Neurosci.* **19:** 133–146.

Peach, R.J., Hollenbaugh, D., Stamenkovic, I., and Aruffo, A. 1993. Identification of hyaluronic acid binding sites in the extracellular domains of CD44. *J. Cell Biol.* **122:** 257–264.

Powell, U.C., Fingleton, B., Wilson, C.L., Boothby, M., and Matrisian, L.M. 1999. The metalloproteinase matrilysin proteolytically generates active soluble Fas ligand and potentiates epithelial cell apoptosis. *Curr. Biol.* **9:** 1441–1447.

Prenzel, N., Zwick, E., Daub, H., Leserer, M., Abraham, R., Wallasch, C., and Ullrich, A. 1999. EGF receptor transactivation by G-protein-coupled receptors requires metalloproteinase cleavage of proHB-EGF. *Nature* **402:** 884–888.

Raab, G., Kover, K., Paria, B.C., Dey, S.K., Ezzell, R.M., and Klagsbrun, M. 1996. Mouse preimplantation blastocysts adhere to cells expressing the transmembrane form of heparin-binding EGF-like growth factor. *Development* **122:** 637–645.

Roach, M.L., Stock, J.L., Byrum, R., Koller, B.H., and McNeish, J.D. 1995. A new embryonic stem cell line from DBA/llacJ mice allows genetic modification in a murine model of human inflammation. *Exp. Cell Res.* **221:** 520–525.

Roca, X., Mate, J.L., Ariza, A., Munoz-Marmol, A.M., von Uexkull-Guldeband, C., Pellicer, I., Navas-Palacios, J.J., and Isamat, M. 1998. CD44 isoform expression follows two alternative splicing pathways in breast tissue. *Am. J. Pathol.* **153:** 183–190.

Rudolph-Owen, L.A., Hulboy, D.L., Wilson, C.L., Mudgett, J., and Matrisian, L.M. 1997. Coordinate expression of matrix metalloproteinase family members in the uterus of normal, matrilysin-deficient and stromelysin-1-deficient mice. *Endocrinology* **138:** 4902–4911.

Rudolph-Owen, L.A., Chan, R., Muller, W.J., and Matrisian, L.M. 1998. The matrix metalloproteinase matrilysin influences early-stage mammary tumorigenesis. *Cancer Res.* **58:** 5500–5506.

Saarialho-Kere, U.K., Crouch, E.C. and Parks, W.C. 1995. Matrix metalloproteinase matrilysin is constitutively expressed in adult human exocrine epithelium. *J. Invest. Dermatol.* **105:** 190–196.

Schneider, P., Holler, N., Bodmer, J.L., Hahne, M., Frei, K., Fontana, A., and Tschopp, J. 1998. Conversion of membrane-bound Fas(CD95) ligand to its soluble form is associated with downregulation of its proapoptotic activity and loss of liver toxicity. *J. Exp. Med.* **187:** 1205–1213.

Screaton, G.R., Bell, M.V., Jackson, D.G., Cornelis, F.B., Gerth, U., and Bell, J.I. 1992. Genomic structure of DNA encoding the lymphocyte homing receptor CD44 reveals at least 12 alternatively spliced exons. *Proc. Natl. Acad. Sci.* **89:** 12160–12164.

Sellers, A. and Woessner, J.F. 1980. The extraction of a neutral metalloproteinase from the involuting rat uterus, and its action on cartilage proteoglycan. *Biochem. J.* **189:** 521–531.

Shapiro, S.D. 1998. Matrix metalloproteinase degradation of extracellular matrix: Biological consequences. *Curr. Opin. Cell Biol.* **10:** 602–608.

Sherman, L., Wainwright, D., Ponta, H., and Herrlich, P. 1998. A splice variant of CD44 expressed in the apical ectodermal ridge presents FGF-8 to limb mesenchyme and is required for limb outgrowth. *Genes & Dev.* **12:** 1058–1071.

Stamenkovic, I., Aruffo, A., Amiot, M., and Seed, B. 1991. The hematopoietic and epithelial forms of CD44 are distinct polypeptides with different adhesion potentials for hyaluronate-bearing cells. *EMBO J.* **10:** 343–348.

Suzuki, M., Raab, G., Moses, M.A., Fernandez, C.A., and Klagsbrun, M. 1997. Matrix metalloproteinase-3 releases active heparin-binding EGF-like growth factor by cleavage at a specific juxtamembrane site. *J. Biol. Chem.* **272:** 31730–31737.

Sweeney, C., Lai, C., Riese II, D.J., Diamonti, A.J., Cantley, L.C., and Carraway, K.L. 2000. Ligand discrimination in signaling through ErbB4 receptor homodimer. *J. Biol. Chem.* **275:** 19803–19807.

Sy, M.S., Guo, Y.J., and Stamenkovic, I. 1991. Distinct effects of two CD44 isoforms on tumor growth in vivo. *J. Exp. Med.* **174:** 859–866.

Vu, T.H. and Werb, Z. 2000. Matrix metalloproteinases: Effectors of development and normal physiology. *Genes & Dev.* **14:** 2123–2133.

Werb, Z. 1997. ECM and cell surface proteolysis: Regulating

cellular ecology. *Cell* **91:** 439–442.
Wilson, C.L. and Matrisian, L.M. 1996. Matrilysin: An epithelial matrix metalloproteinase with potentially novel functions. *Int. J. Biochem. Cell Biol.* **28:** 123–136.
Wilson, C.L., Heppner, K.J., Rudolph, L.A., and Matrisian, L.M. 1995. The metalloproteinase matrilysin is preferentially expressed by epithelial cells in a tissue-restricted pattern in the mouse. *Mol. Biol. Cell* **6:** 851–869.
Wilson, C.L., Heppner, K.J., Labosky, P.A., Hogan, B.L., and Matrisian, L.M. 1997. Intestinal tumorigenesis is suppressed in mice lacking the metalloproteinase matrilysin. *Proc. Natl. Acad. Sci.* **94:** 1402–1407.
Wilson, C.L., Ouillette, A.J., Satchell, D.P., Ayabe, T., Lopez-Boado, Y.S., Stratman, J.L., Hultgren, S.J., Matrisian, L.M., and Parks, W.C. 1999. Regulation of intestinal α-defensin activation by the metalloproteinase matrilysin in innate host defense. *Science* **286:** 113–117.
Witty, J.P., McDonnell, S., Newell, K., Cannon, P., Navre, M., Tressler, R., and Matrisian, L.M. 1994. Modulation of matrilysin levels in colon carcinoma cell lines affects tumorigenicity *in vivo*. *Cancer Res.* **54:** 4805–4812.
Woessner, J.F. 1996. Regulation of matrilysin in the rat uterus. *Biochem. Cell Biol.* **74:** 777–784.
Woessner, J.F. and Taplin, C.J. 1988. Purification and properties of a small latent matrix metalloproteinase of the rat uterus. *J. Biol. Chem.* **263:** 16918–16925.
Wolffe, E.J., Gause, W.C., Pelfrey, C.M., Holland, S.M., Steinberg, A.D., and August, J.T. 1994. The cDNA sequence of mouse Pgp-1 and homology to human CD44 cell surface antigen and proteoglycan core/link proteins. *J. Biol. Chem.* **265:** 341–347.
Yu, Q. and Stamenkovic, I. 2000. Cell surface-localized matrix metalloproteinase-9 proteolytically activates TGF-β and promotes tumor invasion and angiogenesis. *Genes & Dev.* **14:** 63–176.
Yu, W-H. and Woessner, J.F., Jr. 2000. Heparan sulfate proteoglycans as extracellular docking molecules for matrilysin (Matrix metalloproteinase 7). *J. Biol. Chem.* **275:** 4183–4191.